Optics and Lasers in Engineering 107 (2018) 28–37

Contents lists available at ScienceDirect

Optics and Lasers in Engineering

journal homepage: www.elsevier.com/locate/optlaseng

Absolute phase retrieval methods for digital fringe projection profilometry: A review

Song Zhang

School of Mechanical Engineering, Purdue University, West Lafayette, Indiana 47907, USA

ARTICLE INFO

Keywords:
Phase unwrapping
3D shape measurement
Structured light
Fringe projection
Absolute phase

ABSTRACT

This paper provides a review for absolute phase recovery methods that are applicable for digital fringe projection (DFP) systems. Specifically, we present two conventional absolute phase unwrapping methods: multi-frequency or -wavelength phase-shifting methods, and hybrid binary coding and phase-shifting methods; and also introduce some non-conventional methods that are specific for DFP systems: multiview geometry methods with additional camera(s) or projector(s), DFP system geometric constraint-based phase unwrapping method, and pre-knowledge (e.g., computer-aided-design, CAD, model) based phase unwrapping method. This paper also briefly overviews hybrid methods including phase coding, composite, and pre-defined markers based absolute phase unwrapping methods. This paper explains the principle behind each individual absolute phase unwrapping method; and finally offers some practical tips to handle common phase unwrapping artifact issues.

1. Introduction

Three-dimensional (3D) optical shape measurement becomes increasing important due to the ever-growing analytic capabilities of personal computers and nowadays even mobile devices. As a non-contact and remote sensing means, the real-time 3D optical shape measurement techniques have the great potential to be an integrated part of intelligent systems (e.g., machines, robots) [1], as well as to be a novel sensing means for human–machine or human–computer interactions [2].

Digital fringe projection (DFP) based 3D optical shape measurement techniques draw significant interests in various fields because of the flexibility of fringe generation nature, relatively inexpensive and easy setup, and the facilitation by affordable digital-light-processing (DLP) developmental kits [3]. For all DFP-based 3D shape measurement techniques, phase unwrapping is critical since only wrapped phase ranging from $-\pi$ to $+\pi$ can be obtained through analyzing fringe pattern(s) either using a phase-shifting algorithm [4] or a Fourier transform method [5,6]. To unwrap phase, 2π discontinuous locations have to be identified and removed by adding or subtracting multiple integer numbers of 2π. The number of 2π to be added to a point (x, y) is often called fringe order $k(x, y)$. Essentially, phase unwrapping is to determine $k(x, y)$ for each point such that the wrapped phase can be properly unwrapped.

Although numerous phase unwrapping algorithms have been developed, conventional phase unwrapping methods can be classified into two categories: spatial phase unwrapping and temporal phase unwrapping. The former methods unwrap the phase by referring phase values of other points on the same phase map through a local or global optimization. The book edited by Ghiglia and Pritt [7] summarized a number of spatial phase unwrapping methods. Due to the existence of noise, surface reflectivity variations, and other factors, spatial phase unwrapping can be very challenging. Despite recent advancements, robustly unwrapping the entire phase map is still very challenging if the phase data is very noisy. One of the most popular, robust and efficient spatial phase unwrapping methods is to use a quality map to guide the unwrapping path. The basic idea of quality-guided phase unwrapping is that higher quality phase points are unwrapped before lower quality phase points such that the error will not propagate to a lot of points. Su and Chen [8] reviewed a number of robust quality-guided phase unwrapping algorithms, and Zhao et al. [9] compared different strategies of generating a quality map for robust phase unwrapping. Regardless the robustness of a spatial phase unwrapping algorithm, it is fundamentally limited by the surface *smooth* assumption: the object surface has to be smooth to at least one unwrapping path such that the object surface geometry will not introduce more than π phase changes between two successive points. In general, spatial phase unwrapping only provides a relative phase map for a smoothly connected patch. In other words, the recovered shape from a spatially unwrapped phase map is relative to a 3D point on the surface. The absolute position between different smooth patches cannot be recovered.

Temporal phase unwrapping, in contrast, determines fringe order $k(x, y)$ per point based on analyzing additionally acquired information at a temporally different time. In this method, fringe order is determined

E-mail address: szhang15@purdue.edu

https://doi.org/10.1016/j.optlaseng.2018.03.003
Received 29 January 2018; Received in revised form 1 March 2018; Accepted 5 March 2018
0143-8166/

from additionally acquired information without requiring the knowledge of phase values of other points on the phase map, and thus a temporal phase unwrapping method typically yields the absolute fringe order and the unwrapped phase is absolute. Conventional temporal phase unwrapping methods (e.g., two and multi-wavelength phase-shifting algorithms [10,11]) originated from laser interferometry can be directly applied to DFP profilometry. For a noise-free system, a two-wavelength phase-shifting algorithm theoretically works well, yet a practical measurement system always has noise and thus multi-wavelength phase-shifting algorithm is typically required for absolute phase recovery. Creath [12] analyzed the noise impact of two-wavelength phase-shifting methods; Towers et al. [13] proposed the strategies to select optimal wavelengths to minimize the noise influence; and recently Zuo et al. [14] thoroughly studied the problems associated with implementing such temporal phase unwrapping methods to DFP systems.

Unlike laser interferometry where only sinusoidal fringe patterns can be generated, DFP system can generate different forms of structured patterns, enabling a lot more methods for absolute phase unwrapping. For example, fringe order can be directly encoded into a sequence of binary [15,16] or ternary [17] coded patterns, a single statistical pattern [18,19], a single stair image [20], as well as other forms [21–29]. These enriched temporal phase unwrapping methods offer one to select the most suitable phase unwrapping approach for a specific application.

The aforementioned temporal phase unwrapping methods can all work on a single-projector and single-camera DFP system by acquiring additional information (i.e. images). For high-speed applications, it is not desirable to capture additional images since it slows down the entire measurement process. Recently, because of the reduced costs of hardware (e.g., cameras) and the desired high measurement speeds, researchers have developed alternative absolute phase unwrapping methods [30–37] by integrating more hardware components (e.g., a camera or a projector) into the measurement system. Different from a stereo-view system with a single camera and a single projector, these systems typically construct a multiview system that consists of more than two different perspectives. Such a system is over-constrained for 3D reconstruction, providing the opportunity to directly use wrapped phase for absolute 3D shape measurement. Therefore, the additional hardware-based phase unwrapping method has emerged as one of the important absolute phase unwrapping methods. Instead of capturing additional images, this type of phase unwrapping method determines absolute fringe order using the additional geometric constraints available to the hardware system, the wrapped phase constraint, and/or the existing stereo-vision approaches. Since no additional images are required, these absolute phase unwrapping methods do not belong to the conventional temporal phase unwrapping category yet still obtain absolute phase maps. Furthermore, because no additional image acquisition is required, they are more suitable for high-speed applications than the conventional temporal phase unwrapping methods.

In addition to the aforementioned absolute phase unwrapping methods, there are also other absolute fringe order determination methods that were recently developed based on the available information obtained elsewhere. For example, nowadays, most fabricated parts have computer-aided design (CAD) models, and the CAD model can also be used to determine absolute fringe order $k(x, y)$ by sampling the CAD from the same perspective of the camera of the DFP system [38]. We call this type of method *pre-knowledge-based phase unwrapping*. Since the calibrated DFP system provides the geometric relationship between (x, y, z) coordinates and the phase on the projector, An et al. [39] developed the geometric-constraint based phase unwrapping method for the single camera and single projector DFP system, and Jiang et al. [40] extended the depth range of An's method. These methods do not belong to the conventional temporal phase unwrapping category since they do not require temporally acquired information for absolute fringe order determination. Different from the multiview methods, these methods can be applied to a standard single-camera and single-projector DFP system, making them more valuable to high-speed applications at reduced complexity and cost of the hardware system.

This paper reviews conventional and recently emerged absolute phase recovery methods that are applicable to DFP systems. We will thoroughly explain two conventional absolute fringe order determination methods: different frequency phase shifting and binary coding; and discuss some newly emerged major absolute phase recovery methods for DFP systems including multiview geometry-based method by additional more hardware components (e.g., the second camera), the inherent geometric constraint-based method, and pre-knowledge-based method. We will also introduce other methods including hybrid methods such as phase coding, random pattern encoding, as well as the use of pre-defined markers. The principle behind each individual methods will be explained. Furthermore, due to noise and sampling, all absolute phase unwrapping methods create artifacts (i.e., points that are incorrectly unwrapped), they have to be properly handled for practical accurate measurements. This paper will offer some tips on handling those artifacts. Finally, we will cast our perspectives on their difficulty level for implementation.

Section 2 explains principles of each phase unwrapping method. Section 3 discusses some methods to handle phase unwrapping artifacts, and Section 4 summarizes this paper.

2. Principles

2.1. Basics of absolute phase unwrapping

The general sinusoidal fringe pattern can be mathematically represented as

$$I_i(x, y) = I'(x, y) + I''(x, y)\cos(\phi(x, y) + \delta_i), \tag{1}$$

where $I'(x, y)$ is the average intensity, $I''(x, y)$ is the intensity modulation, $\phi(x, y)$ is the phase, and δ_i is the phase shift. To recover phase $\phi(x, y)$, a Fourier transform [5,6] or a phase-shifting method [4] can be employed. Essentially, these algorithms use an arctangent function to compute phase value pixel by pixel. Due to the use of an arctangent function, the resultant phase value ranges from $-\pi$ to $+\pi$, or 0 to 2π with 2π modulus; and the phase obtained at this stage is often called wrapped phase. The wrapped phase has to be unwrapped before being converted to 3D coordinates pixel by pixel. Phase unwrapping is to determine 2π discontinuous locations, find the integer number of 2π's that a point should be added, and then remove 2π discontinuities by adding the desired number of 2π to the wrapped phase, $\phi(x, y)$. Mathematically, the relationship between wrapped phase $\phi(x, y)$ and unwrapped phase, $\Phi(x, y)$ can be described as

$$\Phi(x, y) = k(x, y) \times 2\pi + \phi(x, y). \tag{2}$$

Here $k(x, y)$ is an integer number that is often regarded as *fringe order*. If fringe order $k(x, y)$ can be uniquely determined for each point that is consistent with a pre-defined value, then the unwrapped phase $\Phi(x, y)$ is regarded as *absolute* phase.

As discussed in Section 1, spatial phase unwrapping determines fringe order $k(x, y)$ that is typically relative to one point on the phase, and thus cannot give absolute phase. In contrast, the absolute phase unwrapping determines absolute fringe order $k(x, y)$ by referring to information acquired from somewhere else (e.g., additional images) and thus yields absolute phase.

The remaining sections discuss some of the major absolute fringe order $k(x, y)$ determination methods that can be applicable to the DFP systems. We will explain the basic principles of some well-known conventional methods (e.g., temporal phase unwrapping), and some non-conventional methods.

2.2. Binary coding method

The most straightforward method is to directly encode the fringe order $k(x, y)$ into a sequence of binary structured patterns. And the method

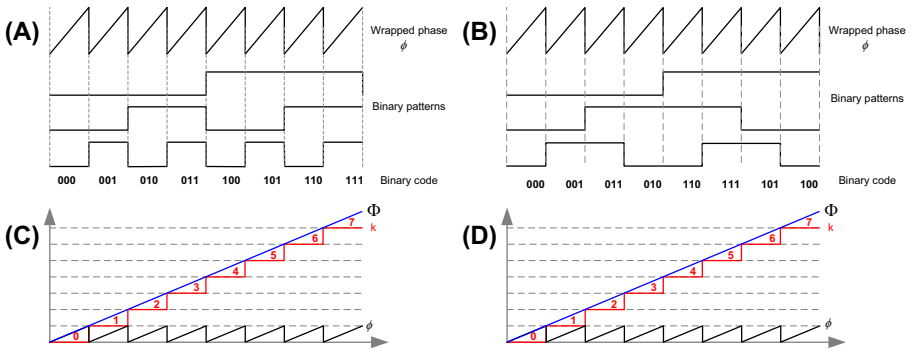

Fig. 1. Example of using binary coded patterns for fringe order determination. (A) Example of binary patterns using simple binary coding and associated wrapped phase ϕ; (B) example of binary patterns using gray coding and associated wrapped phase ϕ; (C) phase unwrapping using fringe order k determined from simple coded binary patterns and (D) phase unwrapping using fringe order k determined from gray coded binary patterns.

of combining the binary coding method with phase-shifting method is often regarded as a hybrid method [15]. Theoretically, all binary coding methods [41] developed for binary structured light 3D shape measurement systems can be adopted. These coding methods could be simple coding [16], stripe boundary coding [42], gray coding [43], modified coding [44], or any space-time coding method [45], along with others. The difference among these coding methods lies in the robustness of handling high-contrast or highly complex object surfaces, as well as the reliability to locate the boundary of binary structured patterns.

Fig. 1 illustrates two coding methods (simple coding and gray coding). As indicated in this figure, the codeword changes coincident with the 2π discontinuous locations of the phase map. If the binary code sequence is determined from the binary structured patterns, the fringe order can be uniquely determined, and thus the phase can be unwrapped pixel by pixel.

Comparing with simple coding, the gray coding is more robust to sampling related problems since at any given phase discontinuous location, only one binary pattern changes its binary state (from 0 to 1 or from 1 to 0), and the coding error can only be introduced by one image. In contrast, the simple coding method can have multiple binary patterns change their states, leading to the coding error introduced by multiple images.

The binary coding-based fringe order determination methods are extensively employed, and they can work pretty well for pseudo-static objects. However, when an object is moving during data acquisition, the motion could cause phase unwrapping problems even if the gray coding method is used. In general, a computational framework is required to properly handle the unwrapping artifacts near the edge of codeword changes. Section 3 will discuss some of the method we found effective to alleviate the unwrapping artifacts.

2.3. Multi-frequency phase-shifting method

Absolute fringe order $k(x, y)$ can be determined for each pixel by referring to phase obtained from fringe patterns with different frequencies, and such a method is often called multi-wavelength or multi-frequency phase-shifting method. The multi-frequency phase-shifting method was originally developed for laser interferometry and is applicable to a DFP system as well. In laser interferometry where fringe patterns are generated by laser interference, the multi-wavelength phase-shifting algorithm refers to use different wavelengths of light sources for fringe pattern generations.

However, in a DFP system, the wavelength of light does not correlate to the fringe patterns used for phase retrieval, it is probably better to use fringe frequency f or fringe period $T = 1/f$ for the sinusoidal fringe patterns generated by a computer. As such, we use multi-frequency phase-shifting algorithm in lien of multi-wavelength phase-shifting algorithm in a DFP system although they are essentially the same.

If we treat fringe period T as the wavelength of light, all mathematical representations of the multi-wavelength algorithm can be directly imported here. In other words, the equivalent fringe period T^{eq} can be written as

$$T^{eq} = \frac{T_1 T_2}{|T_1 - T_2|}, \tag{3}$$

where T_1 and T_2 are fringe periods for two higher frequency fringe patterns, and T^{eq} is the resultant equivalent fringe period if both set of fringe patterns are used to obtain equivalent phase

$$\phi_{12} = [\phi_1 - \phi_2] \mod (2\pi), \tag{4}$$

where ϕ_1 and ϕ_2 are the phase maps obtained from fringe patterns with fringe period of T_1 and T_2, respectively.

By using multiple phase maps with different frequencies, the overall equivalent fringe period can cover the entire fringe projection range, making the equivalent phase to be the *absolute* phase that does not require any phase unwrapping, i.e.,

$$\Phi_{eq}(x, y) = \phi_{eq}(x, y). \tag{5}$$

For the two-frequency case explained above, $\phi_{eq}(x, y) = \phi_{12}$.

This equivalent unwrapped phase can be then used to determine fringe order $k(x, y)$ for the higher frequency phase. For example, if this phase is used to determine fringe order for $\phi_1(x, y)$ with fringe period of T_1, fringe order $k(x, y)$ can be determined by

$$k(x, y) = \frac{\Phi_{eq}(x, y) \times T_{eq}/T_1 - \phi_1}{2\pi}. \tag{6}$$

This step is often referred as *backward phase unwrapping*. Fig. 2 graphically illustrates the multi-frequency fringe order determination method.

Due to the influence of noise, more than two frequencies of phase-shifted fringe patterns are typically used. To increase the robustness of fringe order determination, the backward phase unwrapping step is often executed recursively: the final equivalent phase is used to determine the fringe order for the phase with the second longest *equivalent* fringe period, and such unwrapped phase is then used to unwrap the phase with the third longest *equivalent* fringe period, and so on.

Due to the flexibility of DFP technique, one can freely choose any fringe period T in pixels as long as it is an integer number (Note: integer numbers are used to avoid sub-pixel fringe period representation error); and thus the equivalent phase can be directly obtained by projecting fringe patterns with the equivalent fringe period. And also due to this flexility, the DFP technique allows the use of equivalent fringe period that is difficult to be realized by laser interferometers (for example, the projector can project fringe patterns with one fringe covering the entire fringe period. Therefore, it allows the use of two-frequency phase-shifting algorithm for full range absolute phase unwrapping [29,46,47], albeit the noise could bring challenges [12].

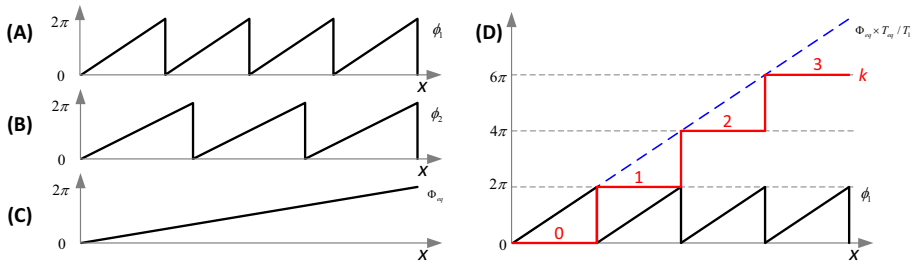

Fig. 2. Illustration of two-frequency algorithm for fringe order determination. (A) and (B) Two frequency phase maps ϕ_1 and ϕ_2; (C) equivalent phase map ϕ_{eq} is also regarded unwrapped phase, Φ, since its phase value ranges from 0 to 2π and (D) fringe order k determination with scaled equivalent phase map.

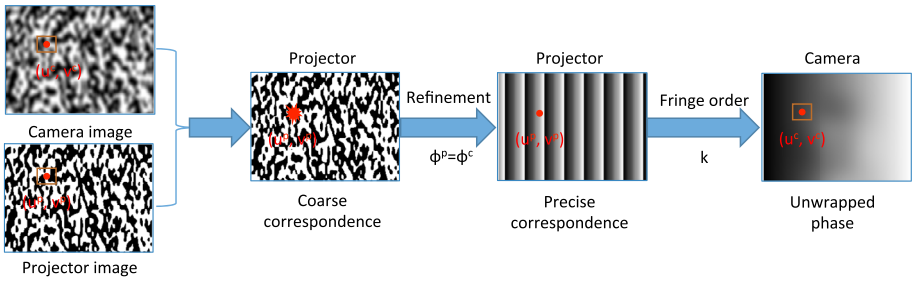

Fig. 3. Framework of using a single statistically random pattern for fringe order determination [18]. For any point (u^c, v^c) on the camera, a small region is selected from the camera captured random pattern to find the corresponding region on the projected random pattern whose center will be the matching point on the projector (u^p, v^p). This matching point is not precise and thus a refinement stage is used to more precisely locate the matching point using the wrapped phase constraint $\phi^c = \phi^p$. After refinement, the fringe order for the wrapped phase at (u^c, v^c) can be determined from projector's matching point (u^p, v^p).

2.4. Statistical pattern based method

The aforementioned temporal phase unwrapping methods need several additional images to determine absolute fringe order. For high-speed applications, it is desirable to reduce the number of patterns used. Therefore, instead of using several grayscale patterns to encode fringe order, $k(x, y)$, one can use a single statistical random pattern. The basic idea is that the projector projects one additional random pattern, and employ a stereo matching method to find the coarse disparity map between the projected image and the camera captured image. Numerous random pattern-based stereo-matching algorithms have been proposed for conventional active stereo-vision systems [48,49], albeit they have been used for the final disparity calculation rather than as an intermediary to matching phase. The Efficient LArge-scale Stereo (ELAS) algorithm [50] could be used to obtain an initial coarse disparity map. Once this coarse disparity map is determined, each camera pixel (u^c, v^c) roughly correlates to one projector point (u^p, v^p). Since the projector point is well defined, the fringe order can be determined. Because statistical pattern does not provide precise pixel level matching, the determined fringe order based on this random image is not precisely aligned with 2π discontinuous locations on the phase map. Therefore, a refinement procedure is required to adjust the misalignment. The refinement stage uses the wrapped phase ϕ as a constraint to slightly adjust the position along the phase changing direction on the projector space (e.g., move u^p left or right if the projected fringe pattern is along v^p direction). Once u^p is determined, fringe order $k(x, y)$ can be determined. Fig. 3 shows the framework of this random pattern based fringe order determination method.

Fig. 4(a) shows an example statistically random pattern that we used for our research. This random pattern, I_p is generated with an intensity value $0 < I_p(x, y) < 255$. Here $I_p(x, y)$ and the random pattern follows the band-limited $1/f$ noise

$$\frac{1}{20 \text{ pixels}} < f < \frac{1}{5 \text{ pixels}}. \tag{7}$$

This pipeline works well in theory. However, to fully take advantage of all software tools developed in computer vision community, it is desirable to make sure images acquired from two different perspectives should be as close as possible (e.g., pixel size is the same, distortion looks similar). Unfortunately, a standard DFP system usually does not satisfy the standard stereo assumptions: (1) it is difficult to match the projector pixel size with the camera pixel size because of different optics and different manufacturers; and (2) the projector image is ideal without being impacted by the object surface texture. To address these problem, An and Zhang [18] have developed a computational framework that essentially involves camera random pattern binarization, projector image rectification and scaling and down or up sampling if necessary. The method can work well, albeit requires very sophisticated algorithms to be able to generate reasonable quality data.

Alternatively, to alleviate the different pixel size problem of the projector and the camera, the second camera can be introduced, as many structured light systems do. The next section will discuss the method using two cameras to determine fringe order for absolute phase unwrapping.

2.5. Stereo vision based method

By adding a second camera, the DFP system becomes an over-constrained system that can be leveraged for fringe order determination. Since two cameras are used, the passive stereo (camera–camera pair) subsystem can be used to unwrap phase for the entire active DFP system if a standard stereo-vision approach can successfully reconstruct the 3D shape. However, it is well known that the passive stereo does not work well for object with low surface texture. Therefore, to increase the robustness of the stereo-vision, the projector is used to project structured patterns (e.g., random dots [51,52], band-limited random patterns [53], binary-coded patterns [45,54], color structured patterns [55,56], or phase-shifted sinusoidal fringe patterns [57,58]). For such methods, the projected patterns allow unique correspondence for the camera pairs; and thus 3D shape can be recovered. However, to improve

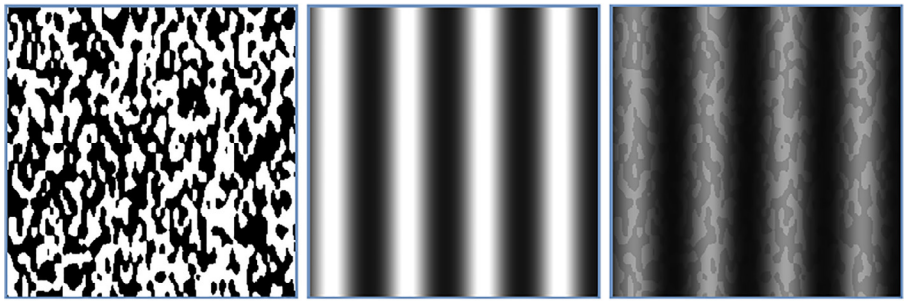

Fig. 4. Example of $1/f$ noise used for statistically random pattern and the associated encoded fringe pattern. (A) Statistically random pattern, $I_p(x, y)$; (B) one of the ideal sinusoidal fringe patterns and (C) modified fringe pattern with encoded random pattern.

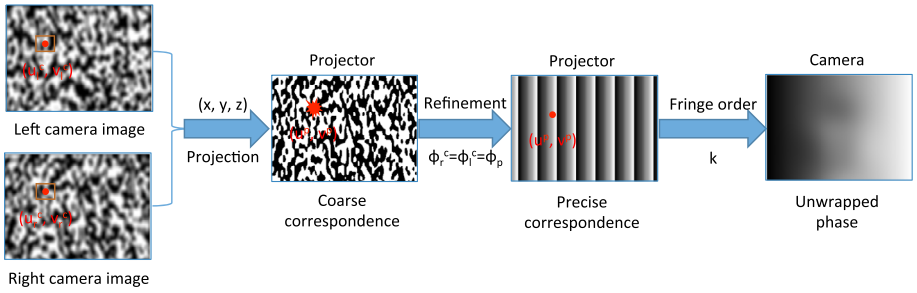

Fig. 5. Framework of the stereo-vision method for fringe order determination. Using the random pattern, the coarse disparity map between the left camera image and the right camera image can be determined. The rough disparity map is further used to reconstruct 3D coordinates for each point. The coarse 3D reconstruction for each point is then projected to the projector sensor space to find the rough location. The rough location can be refined by matching the wrapped phase from the left camera $\phi_l^c(x, y)$ and the right camera $\phi_r^c(x, y)$, and the projector, $\phi^p(x, y)$. The refined corresponding point on the projector provides fringe order $k(x, y)$ for absolute phase unwrapping.

measurement speeds, it is desirable to reduce the number of patterns required for fringe order determination.

One can use a single statistical pattern for active stereo matching, here, such a projected pattern is used to establish correspondence between two cameras. The correspondence based on the random pattern only provides coarse disparity. The coarse disparity map can be used to reconstruct 3D geometry with low resolution. To improve measurement resolution, the phase information can be used to determine fringe order k for each camera pixel, or refine the coarse disparity map, if projector is not calibrated. The former approach projects the reconstructed rough 3D geometry onto projector's sensor plane. This projection provides a rough location of the corresponding point (u^p, v^p) for camera point (u^c, v^c). In order to more precisely locate the corresponding point on the projector, the wrapped phase can be used as a constraint (i.e., $\phi_l^c = \phi_r^c = \phi^p$), which is the same as discussed in Section 2.4. Once u^p is determined, fringe order k can be determined. Fig. 5 illustrates the pipeline of this stereo-vision based fringe order determination method for a calibrated projector.

For the dual-camera, single-projector DFP system, the projector is not required to be calibrated for 3D reconstruction since the projected fringe pattern can be solely used to provide constraints for precise matching between two cameras. For such a case, the corresponding point can be determined by finding the characteristics of local regions of the statistical pattern to search for a similar region on the projected pattern, similar to the method discussed in Section 2.4. And the precise fringe order can be determined again by using the wrapped phase constraint. Alternatively, we do not directly determine the fringe order, but rather refine the coarse disparity map based on the wrapped phase map from the left camera and the right camera, as the method discussed by Lohry et al. [37]. Such a method is more complicated because it could involve with local phase fitting whose accuracy may not be ensured if the surface geometry changes rapidly.

This method combines the advantages of the stereo approach and the phase-based approach: using a stereo matching algorithm to obtain the *coarse disparity* map that can be used to reconstruct rough 3D geometry and that can be used to find the rough location on the projector (if the projector is calibrated); and using wrapped phase of the camera and the defined phase on the projector to precisely determine fringe order $k(x, y)$. Since this method does not require any geometric constraint imposed by the projector, no projector calibration is required. However, if the projector is not calibrated, precise fringe order determination is often difficult and complex, which may reduce measurement accuracy. Furthermore, since this technique requires three different perspectives projections (two cameras and one projector), the possible measurement areas are smaller than the standard DFP system where only one projector and one camera are used. This is because now, three devices instead of two devices have to "see" a point for such a point to be properly measured.

2.6. Multiview geometric constraint-based method

All aforementioned absolute phase retrieval methods require at least one additional image for absolute phase recovery, which could bring challenges for high-speed applications since the object is assumed to be quasi-static during the acquisition of the desired number of images for 3D reconstruction. Because of the reduced hardware cost and flexibility of accurate system calibration, researchers recently explored methods of purely using additional hardware components for absolute phase unwrapping without the need of acquiring any additional images. Because one more view introduces one more set of constraints, these methods use the additional geometric constraints enforced by additional hardware for absolute fringe order determination.

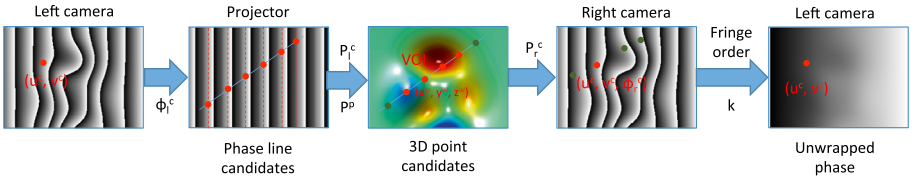

Fig. 6. Multiview geometry for fringe order determination. A point on the left camera with known phase corresponds to a finite discrete number of lines on the projector which can be further used to reconstruct the 3D points (one point per line). These points are regarded as possible candidates, some of which can be rejected if they violate the volume of interest (VOI) condition. The remaining candidate points are projected to the right camera and each point (u^c, v^c) is associated with one phase value, the smallest difference from the right camera phase is regarded as the best candidate point, and is regarded as the true point if the phase difference is smaller than a threshold value. The true point can then be back tracked to find fringe order for phase unwrapping.

The multiview geometry based-absolute phase unwrapping method has been long and extensively studied [30–36]. Such a method uses the wrapped phase, the epipolar geometry, the measurement volume, the phase monotonicity, etc. as constraints to determine the fringe order $k(x, y)$ for each camera pixel and then unwrap the phase without requiring additional images.

Fig. 6 illustrates one possible framework of the trio-geometric constraint-based approach for fringe order determination. Any point on the left camera with a wrapped phase value ϕ_0 corresponds to multiple discrete lines on the projected fringe patterns (e.g., $u_1^p, u_2^p, \ldots$ if the fringe pattern varies along u direction) with exactly the same phase value. If the left camera and the projector are calibrated under the same coordinate system, 3D coordinates (x, y, z) for each candidate can be reconstructed using the line constraint [59]. These 3D points form all possible candidates, and only those candidate points within the volume of interest are considered further. If the right camera and the projector are calibrated under the same coordinate system, these reconstructed 3D points can be projected onto the right camera image plane to determine the corresponding point (u^c, v^c). We then extract the phase value ϕ_{ri}^c for each corresponding point and evaluate difference from the phase on the left camera, $\Delta\phi_i = |\phi_{ri}^c - \phi_0|$. The smallest $\Delta\phi_k$ is then treated as the best candidate. The best candidate will be regarded as the true point if $\Delta\phi_i$ is smaller than a pre-defined threshold value. The true point can then be back tracked to find the fringe order for phase unwrapping.

This method can work well if more global constraints (e.g., phase monotonicity, geometric local smoothness) are checked backward and forward. It is understandable that the more constraints imposed, the more accurate fringe order can be determined, but the more processing time is required. Due to high calibration accuracy requirements for three separate devices (i.e., two cameras and one projector) under exactly the same coordinate system, it is usually not trivial to properly implement this method. Furthermore, again, due to the use of three different perspectives, the possible measurement areas could be reduced since three devices have to "see" a point to perform 3D shape measurement.

2.7. Stereo-view geometric constraint-based method

Instead of using an additional camera, the inherent geometric constraints of a standard DFP system (i.e., a single camera and a single projector) could also be used to determine fringe order for each pixel, and such a method is called minimum phase method [39]. In this method, assume both camera and projector follow the linear pinhole mode and are precisely calibrated under the same world coordinate system. The projections from 3D world coordinate system to 2D sensor plane can be represented as,

$$s^c \begin{bmatrix} u^c & v^c & 1 \end{bmatrix}^t = \mathbf{P^c} \begin{bmatrix} x^w & y^w & z^w & 1 \end{bmatrix}^t, \tag{8}$$

$$s^p \begin{bmatrix} u^p & v^p & 1 \end{bmatrix}^t = \mathbf{P^p} \begin{bmatrix} x^w & y^w & z^w & 1 \end{bmatrix}^t. \tag{9}$$

Here $\mathbf{P}$ denoted 3×4 projection matrix from world coordinates (x^w, y^w, z^w) to sensor 2D image coordinates (u, v), superscript $^\mathbf{p}$ represents projector, superscript $^\mathbf{c}$ presents camera, and ^{t} denotes the transpose operation of a matrix.

The projection matrices, $\mathbf{P^c}$ and $\mathbf{P^p}$ can be estimated through calibration. Therefore, Eqs. (8) and (9) have 6 equations with 7 unknowns $(s^c, s^p, x^w, y^w, z^w, u^p, v^p)$ for each camera pixel (u^c, v^c), and one additional constraint equation is needed to solve all unknowns uniquely. For example, for a DFP system, the absolute phase $\Phi(x, y)$ is often used as a constraint to recover (x^w, y^w, z^w) coordinates [59]. The absolute phase $\Phi(x, y)$ essentially maps one point on the camera image plane (u^c, v^c) to a line, u^p or v^p, on the projector image plane with exactly the same phase value.

In contrast, if a virtual plane at $z = z^w$ is defined, the camera sensor image can be uniquely mapped to a projector sensor region with defined phase value. If $z = z_{min}$, we call the virtually created phase map as minimum phase or Φ_{min} that is a function of z_{min}, fringe period T, and projection matrices, i.e.,

$$\Phi_{min}(u^c, v^c) = f(z_{min}; T, \mathbf{P}^c, \mathbf{P}^p). \tag{10}$$

Fig. 7 illustrates the basic concept of using the minimum phase to determine fringe order. Assume the red dashed window shows the corresponding projector region that the camera captures an ideal plane at $z = z_{min}$. The corresponding Φ_{min} is defined on the projector space and thus is continuous without requiring any phase unwrapping, as shown in Fig. 7(b). For a plane at unknown depth $z > z_{min}$, the camera captured wrapped phase is ϕ, and the corresponding region on the projector is marked as the solid blue window. Fig. 7(c) shows the cross section of these phase maps. Clearly, if $\phi < \Phi_{min}$, fringe order k can be determined as 1, or 2π should also be added to unwrap the phase ϕ.

Fig. 7(d) and (e), respectively, illustrates two and three discontinuous locations. An et al. [39] has proven that, in general, the fringe order $k(x, y)$ can be determined by

$$k(x, y) = ceil\left[\frac{\Phi_{min} - \phi}{2\pi}\right]. \tag{11}$$

Here, *ceil*[] is the ceiling operator that gives the nearest upper integer number.

The geometric constraint-based fringe order determination method has the following advantages [60]: (1) unlike traditional temporal phase unwrapping method, this absolute phase unwrapping method does not require any additional image acquisition, and thus it is more suitable for high-speed applications; and (2) this method is robust to noise because it determines fringe order by referring to an artificially generated ideal absolute phase map Φ_{min} without any noise. In contrast, the conventional temporal phase unwrapping method determines fringe order by referring to camera captured information that contains noise. However, this fringe order determination method has one major limitation: the maximum measurement depth range is within 2π changes in phase domain from the object plane to the minimum phase generation plane. In other words, any point on the object surface should not be too far away from z_{min} such that it will cause more than 2π changes. Assuming the angle between projection direction and camera capture direction is θ, and the spatial span of one projected fringe period is ΔT_s, the maximum

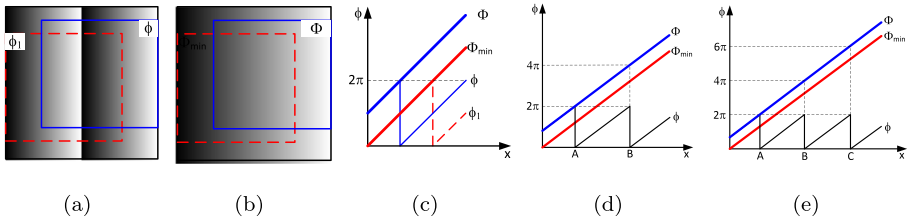

Fig. 7. Conceptual idea of determining fringe order $k(x, y)$ by using minimum phase Φ_{min} obtained from geometric constraints of the DFP system [39]. (a) Red dashed window shows camera captured area when the virtual plane is at $z = z_{min}$ and the solid blue window shows when the virtual plane is at $z > z_{min}$; (b) corresponding Φ_{min} and Φ defined on the projector; (c) cross sections of Φ_{min} and Φ and the wrapped phase maps for the case of only one single 2π discontinuous location; (d) unwrap phase for two discontinuous locations and (e) unwrap phase for three discontinuous locations. (For interpretation of the references to color in this figure legend, the reader is referred to the web version of this article.)

depth range that this method can handle is

$$\Delta z_{max} = z_{max} - z_{min} = \Delta T_s / \tan\theta. \tag{12}$$

Jiang et al. [40] subsequently developed a method to extend the depth sensing range by combining pre known rough topology of the object. This phase unwrapping method can be used to enhance two-frequency phase-shifting method for fringe order determination [61], and can be used to determine fringe order for the phase determined from Fourier method [62] and further to reduce motion induced artifacts [63]. If a pre-known sized object is always within the field of view, this method substantially extends the depth range for dynamic 3D shape measurement [64].

2.8. CAD-model based method

Instead of using a conventional black-box fringe order determination approach, we can also utilize our pre-knowledge of the object to determine fringe order. Modern manufacturing starts with the a compute-aided-design (CAD) model before making the part, and thus the CAD model is available and can be leveraged to simplify measurements. Once CAD model is known, the coordinates on each critical feature points (e.g., corners, edges, etc.) are precisely known, albeit it is defined in its own coordinate system. For example, if one knows the part has a few blocks with known dimensions relative to the base, such information can be taken into consideration for fringe order determination.

Assume a set of feature points with known coordinates in the object coordinate system are (x_i^o, y_i^o, z_i^o), and their corresponding coordinates on the camera image are (u_i^c, v_i^c); and also assume the DFP system is calibrated such that its world coordinates is aligned with the camera lens. We will have the following projection relationship between the 3D point and the 2D image point.

$$s_i^c \begin{bmatrix} u_i^c & v_i^c & 1 \end{bmatrix}^t = \mathbf{P^c} \begin{bmatrix} x_i^w & y_i^w & z_i^w & 1 \end{bmatrix}^t \tag{13}$$

$$= \mathbf{P^c} \cdot \mathbf{T^o} \begin{bmatrix} x_i^o & y_i^o & z_i^o & 1 \end{bmatrix}^t, \tag{14}$$

Here $\mathbf{P^c} \cdot \mathbf{T^o}$ can be obtained by solving the set of linear equations such as through the singular value decomposition (SVD) algorithm. Once $\mathbf{P^c} \cdot \mathbf{T^o}$ is known, the transformation from the object coordinate system to the camera lens coordinate system can be determined by

$$\begin{bmatrix} x_i^w & y_i^w & z_i^w & 1 \end{bmatrix}^t = \mathbf{T^o} \begin{bmatrix} x_i^o & y_i^o & z_i^o & 1 \end{bmatrix}^t. \tag{15}$$

Since $\mathbf{T^o}$ is fixed to the entire object, a set of feature points can be used to determine this matrix that can be applied to all measurement points. Once the transformation matrix is determined, the CAD model coordinate system can be transformed to the world coordinate system of the DFP system. The transformed CAD model is then projected onto camera (u^c, v^c) coordinates for each camera pixel, but the depth information z^w can be preserved, if necessary. Similarly, the CAD can also be projected to the projector's (u^p, v^p) coordinate system for each camera pixel by taking advantage of the available depth z^w information. The mapping at this point may not be precise for real measurement due to measurement error and fabrication error. To precisely establish the correspondence, the real captured phase $\phi^c(x, y)$ from phase-shifted fringe patterns can be used as a constraint to refine the corresponding point on the projector. Once the corresponding point is precisely located, the fringe order can be determined for each camera pixel to unwrap the phase map. Li et al. [38] combined this method with the minimum phase-based method [39] to relax the precise pixel matching requirement.

2.9. Hybrid methods

2.9.1. Phase coding method

As aforementioned, the binary coding + phase-shifting technique is one of the major methods by designing a unique codeword assigned to each 2π phase-change period to determine fringe order $k(x, y)$. However, the maximum number of available unique codeword is limited to 2^M (M is the number of binary patterns used). For example, three binary coded patterns can generate up to 8 unique codewords [21]. In contrast, multi-frequency phase-shifting method has the potential of using three additional fringe patterns for absolute phase recovery pixel by pixel without such a limitation.

If the codewords are embedded into phase domain and carried along with three phase-shifted fringe patterns, more codewords could be generated. Wang and Zhang [21] developed such a method that is called phase coding method. Instead of encoding the codeword into binary intensity images, the codeword is embedded into the phase ranging $[-\pi, +\pi)$ of phase-shifted fringe patterns. Since the codeword is a finite number that can quantify the phase into discrete levels, this technique has the following merits: (1) less sensitive to surface contrast, ambient light, and camera noises because of the use of phase-shifting method; (2) fast measuring speed since it only requires three additional images to determine fringe order larger than 8 (better than a gray coding method).

Other researchers [22–26] have developed variations of the phase coding based method for fringe order determination and some increased the robustness or reduced the number of patterns required. For example, Hyun and Zhang [26] have developed a high speed and large depth range 3D shape measurement that achieved kHz 3D shape measurement with only five fringe patterns. Hyun and Zhang's method combined the phase coding method with the geometric-constraint-based phase unwrapping method to achieve both speed improvement and robustness boost. This is a rather powerful method comparing with intensity-domain binary-coding method for fringe order determination. However, comparing with multi-frequency phase-shifting method, the phase-coding method is more sensitive to defocusing, and it requires a complex computational framework to reduce unwrapping artifacts if the projector is substantially defocused.

2.9.2. Encode random statistical pattern into fringe pattern

The stereo-vision method discussed in Section 2.5 uses one additional statistical pattern for stereo-matching. However, for a DFP system

with dual cameras, the phase quality is not as critical as a standard DFP system (i.e., a single camera and a single projector) since the phase is not directly used for 3D reconstruction, but rather used for stereo constraints. Therefore, to speed up measurement, the statistical pattern can be encoded into the phase-shifted fringe patterns. For example, Lohry et al. [37] modified the intensity modulation $I''(x, y)$ by a statistical weight pattern I_p. Here I_p is randomly generated with an intensity value $0.5 < I_p(x, y) < 1$. Here $I_p(x, y)$ follows the band-limited $1/f$ noise shown in Eq. (7). As a result, the ith phase-shifted fringe pattern in Eq. (1) can be written as

$$I_i(x, y) = I' + I_p(x, y)I'' \cos\left(\phi - \delta_i\right). \tag{16}$$

The rationale of encoding the statistical pattern into intensity modulation is the preserved average intensity $I'(x, y)$, which is often used as texture. Fig. 4 illustrates the encoded pattern $I_p(x, y)$ and one of the modified fringe patterns. Fringe order determination is almost identical to the one discussed in Section 2.5, except the random pattern is obtained by extracting I_p from phase-shifted fringe patterns instead of the directly captured image. Lohry and Zhang subsequently demonstrated that such a method can be further developed to substantially improve measurement speeds by binarizing phase-shifted fringe patterns (e.g., through dithering) [65].

2.9.3. Composite frequency based method

To speed up measurement, researchers [27–29] attempted to combine different frequencies into carrier fringe patterns. The phase for each frequency component can be separated by applying band-pass filters [27,28], or via direct computation using signal demodulation theory [29]. The former could work if these frequency components are distinctly separate. The latter does not have to use band-pass filters for frequency recovery, which is more robust. In either case, these methods sacrifice the contrast to improve speed, which might not be desirable for high accuracy measurement applications.

2.10. Some other methods

2.10.1. Finite gray value encoding

Li et al. [66] proposed a method using a single pattern that only has three grayscale values, 0, 128 and 255, to determine fringe order. The encoded pattern is locally unique and pseudo random for each fringe order. In their implementation, they used three unique slits to represent one grayscale values (0, 128 or 255), and three unique slits to represent two grayscale values (0 and 128, 0 and 255, and 128 and 255). These six unique slits are used to generate a pseudo random sequence by searching a Hamilton Circuit over a direct graph [19] such that it simultaneously satisfies: (1) any subsequence with a given length (window size) should appear only once in the whole sequence; and (2) there are no repeated unique slits in every sequence. This method could work well if the object surface is rather smooth (e.g., a human face). However, the decoding process is quite complex and time consuming: involving complicated additional image processing to reduce the impact of surface contrast variations, also voting to address missing/incorrect coded information due to object occlusions or image noise.

Zhang [20] used a stair image (more grayscale values) to directly encode fringe order into different grayscale values. If the surface reflectivity is quite uniform, this approach is very simple to be realized and works really well. The method has been demonstrated its success for relatively complex 3D shape measurements by developing a quite sophisticated computational framework. However, this approach is sensitive to noise of the hardware, surface reflectivity variations, and lens defocusing etc. For example, we have found that this method does not work well for high-contrast surfaces since the low reflective points have very high noise or low signal to noise ratio (SNR) that fail the entire algorithm.

2.10.2. Marker based methods

Single or multiple marker points or stripe(s) [67–74] have also been used to determine absolute fringe order by combining with spatial phase unwrapping methods for absolute phase recovery. The basic assumption is that the spatial phase unwrapping can properly unwrap the phase for each region. It is well known that conventional spatial phase unwrapping cannot determine absolute fringe order. However, if a marker with a known fringe order is determined for that region or the starting point is strategically encoded with a marker [67], the relative unwrapped phase can be adjusted by shifting the entire region phase to ensure the marker point has correct fringe order information. This method can work well if two conditions are simultaneously satisfied: (1) the surface can be segmented into smooth regions, and for each region, a spatial phase unwrapping can successfully unwrap the entire phase; and (2) the encoded marker is clearly visible and accurately determined for each labelled region. The limitations of these approaches are obvious: (1) the method fails if one of the conditions violates; (2) the spatial phase unwrapping is typically slow; and (3) no high quality measurement can be achieved for those marked points.

3. Unwrapping artifacts reduction

The absolute fringe order determination methods discussed in this paper could lead to five following major artifacts: (1) points with incorrect fringe orders are sparsely distributed; (2) points with incorrect fringe orders are on object boundary; (3) points with incorrect fringe orders are densely distributed within the phase map; (4) points with incorrect fringe orders are clutched and those clutches are sparsely distributed; and (5) missing points or regions. There are numerous algorithms to identify the incorrectly determined fringe order points and some attempted to fix them [14,75–84]. They can all work well under certain situations, and reduce unwrapping artifacts to a certain degree for most cases. However, these algorithms were mainly developed to handle the artifacts created from multi-frequency phase-shifting algorithms. And if the fringe order is determined from a different method, such as stereovision, the effectiveness of these algorithms could be drastically reduced due to different characteristics of the artifacts. To our knowledge, none of the existing algorithms works very well for all different types of artifacts, albeit they can all alleviate the problems to a certain level. This section discusses some practices that we found effective and efficient to reduce unwrapping artifacts.

3.1. Sparse artifact points

Sparse point artifact is characterized as incorrect points with 1- or 2-pixel width and distributed sparsely on the measurement surface. This type of artifacts occur in almost all temporal phase unwrapping methods, especially for multi-frequency phase unwrapping methods when the phase quality is rather high. This type of artifact is similar to "*salt and pepper*" noise on 2D images, and is thus quite easy to handle: we found that one of the most effective methods was to apply median filter to locate those incorrectly unwrapped points, and then determine the fringe order differences by comparing the filtered phase $\Phi_m(x, y)$ and the raw phase $\Phi(x, y)$,

$$\Delta k(x, y) = \text{Round}\left[\frac{\Phi_m(x, y) - \Phi(x, y)}{2\pi}\right]. \tag{17}$$

Here *Round*() is an operator that determines the closest integer numbers for a value. $\Delta k(x, y) \neq 0$ indicates point (x, y) has incorrect fringe order which can be corrected by

$$k_c(x, y) = k(x, y) + \Delta k(x, y). \tag{18}$$

Due to its simplicity, such a method can be easily implemented onto the graphics processing unit (GPU) for efficient artifacts reduction [47]. It should be noted that this approach only corrects those artifact points but does not smooth the phase as standard median filtering does.

3.2. Boundary artifacts

This type of artifacts is characterized as those incorrect points appear between the object and the background or on the edge of abruptly changing edges of the object. It is a very common type of artifacts due to the nature of optics. This type of artifacts are typically not very difficult to handle. One of the common approach is to compute phase gradient

$$\nabla\Phi(x,y)=\left[\frac{\partial\Phi(x,y)}{\partial x},\frac{\partial\Phi(x,y)}{\partial y}\right], \tag{19}$$

and a point is regarded as an artifact point if

$$\left[\frac{\partial\Phi(x,y)}{\partial x}\right]^2+\left[\frac{\partial\Phi(x,y)}{\partial y}\right]^2>\epsilon. \tag{20}$$

Here, ϵ is a predefined threshold. Alternatively, one can compute the Laplacian of the unwrapped phase as

$$\nabla^2\Phi(x,y)=\Delta\Phi(x,y)=\left[\frac{\partial^2\Phi(x,y)}{\partial x^2},\frac{\partial\Phi(x,y)^2}{\partial y^2}\right], \tag{21}$$

similarly, identify the a point as an artifact point by satisfying the following condition:

$$\left[\frac{\partial\Phi(x,y)^2}{\partial x^2}\right]^2+\left[\frac{\partial\Phi(x,y)^2}{\partial y^2}\right]^2>\epsilon. \tag{22}$$

Typically, this method can only locate one or two pixel wide artifacts on the boundary, and simply removing these points should not bring too much concerns. If one would like to remove more than a few pixels from the boundary, the image erosion technique developed in machine vision can be adapted for this purpose. However, it should be noted that, this approach can also effectively identify the sparse artifact points. Once these artifact points are located, they can be replaced by approximating the value with neighboring pixel phase information. These approximated value can then be regarded as the filtered phase value Φ_m, and then adjusted using the method discussed in the previous section. Therefore, this method cannot only identify but also has the potential to fix those incorrect fringe orders.

3.3. Dense point artifact

This type of artifacts is characterized as a lot of incorrectly unwrapped points distributed densely on the object surface. It again typically appears on the conventional temporal phase unwrapping methods, especially a small number of frequencies are used for the multi-frequency phase-shifting methods discussed in Section 2.3. Our study found that one of the most effective methods to reduce this type of noise influence is applying Gaussian filter for each wrapped phase computation (i.e., filtering equivalent sine and cosine terms before applying the inverse tangent for phase calculation), and then determining fringe order from the filtered wrapped phase maps. The original phase map without filtering can then be unwrapped. This step typically greatly reduces the number of artifact points on the unwrapped phase map, and most probably leads to the sparsely distributed artifact points that can be handled by the approach discussed in Section 3.1. If the artifacts still cannot be properly handled, the data quality might be too low (e.g., SNR is too low) for high-quality measurements.

3.4. Sparse clutched artifact

This type of artifacts is characterized as a lot of incorrectly unwrapped points connected together, that is, the entire subregion is wrong. This type of artifacts appears on a multiview or even stereo-view system when a stereovision algorithm is applied, especially when dense fringe patterns are used; and it sometimes occurs on temporally unwrapped phase as well if the object moves during data acquisition. Apparently, this type of artifacts is very difficult to handle. Typically, one has to apply an adaptive computational framework for each case. For example, to reduce motion introduced artifacts, combining spatial phase unwrapping with temporal phase unwrapping can work reasonably well assuming that each object is smooth and can be segmented through analyzing the captured fringe patterns [43,63]. To increase the robustness of the computational framework, one can also use the inherent constraints of the DFP system (e.g., the phase is monotonic [75]), use statistical clustering approach [79], or develop advanced machine learning techniques.

3.5. Missing area

The missing points do not occur often for a conventional temporal phase unwrapping, although they do appear after applying a computational framework for artifact reduction. In contrast, if a conventional stereovision algorithm is used at any stage to find rough fringe order, there are a lot missing points on the stereo algorithm that fails to find corresponding points. To recover those missing points, one can use the already correctly unwrapped phase to fit a smooth curve or surface locally or smoothly, estimate the rough phase value $\bar{\Phi}(x,y)$, map the rough phase value to the projector space to locate the phase line, and then combine with phase refinement approach discussed in Section 2 to precisely determine fringe order for that point and thus the absolute phase value $\Phi(x,y)$ [18].

4. Summary

This paper summarized absolute phase recovery methods that are applicable for digital fringe projection (DFP) systems. We have discussed the conventional absolute phase unwrapping methods, some non-conventional methods that are specific for DFP systems, as well as hybrid methods. This paper explained the basic principle behind each individual method. This paper also presented some practical methods that we found effective to reduce unwrapping artifacts. We hope that this paper will be a good reference paper for students, scientists, and researchers who are interested in employing DFP techniques for absolute 3D shape measurement.

Funding information

National Science Foundation (NSF) (1263236, 0968895 and 1102301).

Supplementary material

Supplementary material associated with this article can be found, in the online version, at doi:10.1016/j.optlaseng.2018.03.003.

References

[1] Li B, An Y, Cappelleri D, Xu J, Zhang S. High-accuracy, high-speed 3D structured light imaging techniques and potential applications to intelligent robotics. Int J Intell Robot Appl 2017;1(1):86–103.
[2] Bell T, Karpinsky N, Zhang S. High-resolution, real-time 3D sensing with structured light techniques. In: Interactive displays: natural human–interface technologies. Hoboken, NJ: John Wiley & Sons; 2014. p. 181–213. Chapter 5.
[3] Zhang S. Recent progresses on real-time 3-D shape measurement using digital fringe projection techniques. Opt Laser Eng 2010;48(2):149–58.
[4] Malacara D, editor. Optical shop testing. 3rd ed., New York, NY: John Wiley and Sons; 2007.
[5] Takeda M, Mutoh K. Fourier transform profilometry for the automatic measurement of 3-D object shapes. Appl Opt 1983;22:3977–82.
[6] Su X, Zhang Q. Dynamic 3-D shape measurement method: a review. Opt Laser Eng 2010;48:191–204.
[7] Ghiglia D C, Pritt M D, editors. Two-dimensional phase unwrapping: theory, algorithms, and software. New York: John Wiley and Sons; 1998.
[8] Su X, Chen W. Reliability-guided phase unwrapping algorithm: a review. Opt Laser Eng 2004;42(3):245–61.
[9] Zhao M, Huang L, Zhang Q, Su X, Asundi A, Kemao Q. Quality-guided phase unwrapping technique: comparison of quality maps and guiding strategies. Appl Opt 2011;50(33):6214–24.
[10] Cheng Y-Y, Wyant JC. Two-wavelength phase shifting interferometry. Appl Opt 1984;23:4539–43.

[11] Cheng Y-Y, Wyant JC. Multiple-wavelength phase shifting interferometry. Appl Opt 1985;24:804–7.
[12] Creath K. Step height measurement using two-wavelength phase-shifting interferometry. Appl Opt 1987;26:2810–16.
[13] Towers DP, Jones JDC, Towers CE. Optimum frequency selection in multi-frequency interferometry. Opt Lett 2003;28:1–3.
[14] Zuo C, Huan L, Zhang M, Chen Q, Asundi A. Temporal phase unwrapping algorithms for fringe projection profilometry: a comparative review. Opt Laser Eng 2016;85:84–103.
[15] Sansoni G, Carocci M, Rodella R. Three-dimensional vision based on a combination of gray-code and phase-shift light projection: analysis and compensation of the systematic errors. Appl Opt 1999;38:6565–73.
[16] Zhang S. Flexible 3D shape measurement using projector defocusing: extended measurement range. Opt Lett 2010;35(7):931–3.
[17] Zheng D, Kemao Q, Da F, Seah HS. Ternary gray code-based phase unwrapping for 3D measurement using binary patterns with projector defocusing. Appl Opt 2017;56(13):3660–5.
[18] An Y, Zhang S. Three-dimensional absolute shape measurement by combining binary statistical pattern matching with phase-shifting methods. Appl Opt 2017;56(19):5418–26.
[19] Li Y, Jin H, Wang H. Three-dimensional shape measurement using binary spatio-temporal encoded illumination. J Opt A Pure Appl Opt 2009;11(7):075502.
[20] Zhang S. Composite phase-shifting algorithm for absolute phase measurement. Opt Laser Eng 2012;50(11):1538–41.
[21] Wang Y, Zhang S. Novel phase coding method for absolute phase retrieval. Opt Lett 2012;37(11):2067–9.
[22] Zhou C, Liu T, Si S, Xu J, Liu Y, Lei Z. Phase coding method for absolute phase retrieval with a large number of codewords. Opt Express 2012;20(22):24139–50.
[23] Zhou C, Liu T, Si S, Xu J, Liu Y, Lei Z. An improved stair phase encoding method for absolute phase retrieval. Opt Laser Eng 2015;66:269–78.
[24] Chen X, Lu C, Ma M, Mao X, Mei T. Color-coding and phase-shift method for absolute phase measurement. Opt Commun 2013;298:54–8.
[25] Xing Y, Quan C, Tay C. A modified phase-coding method for absolute phase retrieval. Opt Laser Eng 2016;87:97–102.
[26] Hyun J, Zhang S. Superfast 3D absolute shape measurement using five fringe patterns. Opt Laser Eng 2017;90:217–24.
[27] Li J-L, Su H-J, Su X-Y. Two-frequency grating used in phase-measuring profilometry. Appl Opt 1997;11:277–80.
[28] Guan C, Hassebrook LG, Lau DL. Composite structured light pattern for three-dimensional video. Opt Express 2003;11:406–17.
[29] Liu K, Wang Y, Lau DL, Hao Q, Hassebrook LG. Dual-frequency pattern scheme for high-speed 3-D shape measurement. Opt Express 2010;18:5229–44.
[30] Zhong K, Li Z, Shi Y, Wang C. Analysis of solving the point correspondence problem by trifocal tensor for real-time phase measurement profilometry. In: Proceedings of the 2012 SPIE international society for optical engineering, 8493; 2012. p. 849311.
[31] Li Z, Zhong K, Li Y, Zhou X, Shi Y. Multiview phase shifting: a full-resolution and high-speed 3D measurement framework for arbitrary shape dynamic objects. Opt Lett 2013;38(9):1389–91.
[32] Zhong K, Li Z, Shi Y, Wang C, Lei Y. Fast phase measurement profilometry for arbitrary shape objects without phase unwrapping. Opt Laser Eng 2013;51(11):1213–22.
[33] Brauer-Burchardt C, Kuhmstedt P, Notni G. Phase unwrapping using geometric constraints for high-speed fringe projection based 3D measurements. In: Proceedings of the 2013 SPIE international society for optical engineering, 8789; 2013. p. 878906.
[34] Ishiyama R, Sakamoto S, Tajima J, Okatani T, Deguchi K. Absolute phase measurements using geometric constraints between multiple cameras and projectors. Appl Opt 2007;46(17):3528–38.
[35] Brauer-Burchardt C, Kuhmstedt P, Heinze M, Kuhmstedt P, Notni G. Using geometric constraints to solve the point correspondence problem in fringe projection based 3D measuring systems. In: Proceedings of the sixteenth international conference on Image analysis and processing, Part II; 2011. p. 265–74.
[36] Huddart YR, Valera JDR, Weston NJ, Moore AJ. Absolute phase measurement in fringe projection using multiple perspectives. Opt Express 2013;21(18):21119–30.
[37] Lohry W, Chen V, Zhang S. Absolute three-dimensional shape measurement using coded fringe patterns without phase unwrapping or projector calibration. Opt Express 2014;22(2):1287–301.
[38] Li B, Bell T, Zhang S. Computer-aided-design (CAD) model-assisted absolute three--dimensional shape measurement. Appl Opt 2017;56(24):6770–6.
[39] An Y, Hyun J-S, Zhang S. Pixel-wise absolute phase unwrapping using geometric constraints of structured light system. Opt Express 2016;24(15):18445–59.
[40] Jiang C, Li B, Zhang S. Pixel-by-pixel absolute phase retrieval using three phase-shifted fringe patterns without markers. Opt Laser Eng 2017;91:232–41.
[41] Salvi J, Fernandez S, Pribanic T, Llado X. A state of the art in structured light patterns for surface profilometry. Pattern Recognit 2010;43(8):2666–80.
[42] Hall-Holt O, Rusinkiewicz S. Stripe boundary codes for real-time structured-light range scanning of moving objects. Proceedings of the eighth IEEE international conference on computer vision; 2001. pp. II:359–366.
[43] Wang Y, Zhang S, Oliver JH. 3-D shape measurement technique for multiple rapidly moving objects. Opt Express 2011;19(9):5149–55.
[44] Zhang Q, Su X, Xiang L, Sun X. 3-D shape measurement based on complementary gray-code light. Opt Laser Eng 2012;50:574–9.
[45] Davis J, Ramamoorthi R, Rusinkiewicz S. Spacetime stereo: a unifying framework for depth from triangulation. In: Proceedings of the 2003 IEEE computer society conference on computer vision and pattern recognition, 2; 2003. p. 355–66.
[46] Wang Y, Laughner JI, Efimov IR, Zhang S. 3D absolute shape measurement of live rabbit hearts with a superfast two-frequency phase-shifting technique. Opt Express 2013;21(5):5822–32.
[47] Karpinsky N, Hoke M, Chen V, Zhang S. High-resolution, real-time three-dimensional shape measurement on graphics processing unit. Opt Eng 2014;53(2):024105.
[48] Maruyama M, Abe S. Range sensing by projecting multiple slits with random cuts. IEEE Trans Pattern Anal Mach Intell 1993;15(6):647–51.
[49] Konolige K. Projected texture stereo. In: Proceedings of the 2010 IEEE international conference on robotics and automation; 2010. p. 148–55.
[50] Geiger A, Roser M, Urtasun R. Efficient large-scale stereo matching. In: Proceedings of the 2010 Asian Conference on Computer Vision; 2010. p. 25–38.
[51] Zhang Z. Microsoft kinect sensor and its effect. IEEE Multimed 2012;19(2):4–10.
[52] Huang Y, Shang Y, Liu Y, Bao H. Handbook of 3D machine vision: optical metrology and imaging. In: 3D shapes from speckle. CRC; 2013. p. 33–56.
[53] Wiegmann A, Wagner H, Kowarschik R. Human face measurement by projecting bandlimited random patterns. Opt Express 2006;14(17):7692–8.
[54] Zhang L, Snavely N, Curless B, Seitz SM. Spacetime faces: high-resolution capture for modeling and animation. ACM Trans Graph 2004;23(3):548–58.
[55] Zhang L, Curless B, Seitz S. Spacetime stereo: Shape recovery for dynamic scenes. In: Proceedings of the 2003 conference on computer vision and pattern recognition.; 2003. p. 367–74.
[56] Jang W, Je C, Seo Y, Lee SW. Structured-light stereo: comparative analysis and integration of structured-light and active stereo for measuring dynamic shape. Opt Laser Eng 2013;51(11):1255–64.
[57] Schaffer M, Große M, Harendt B, Kowarschik R. Coherent two-beam interference fringe projection for high-speed three-dimensional shape measurements. Appl Opt 2013;52(11):2306–11.
[58] Liu K, Wang Y. Phase channel multiplexing pattern strategy for active stereo vision. In: Proceedings of the 2012 international conference on 3D imaging (IC3D); 2012. p. 1–8.
[59] Zhang S, Huang PS. Novel method for structured light system calibration. Opt Eng 2006;45(8):083601.
[60] An Y, Liu Z, Zhang S. Evaluation of pixel-wise geometric constraint-based phase unwrapping method for low signal-to-noise-ratio (SNR) phase. Adv Opt Technol 2016;5(5–6):423–32.
[61] Hyun J-S, Zhang S. Enhanced two-frequency phase-shifting method. Appl Opt 2016;55(16):4395–401.
[62] Li B, An Y, Zhang S. Single-shot absolute 3D shape measurement with fourier transform profilometry. Appl Opt 2016;55(19):5219–25.
[63] Li B, Liu Z, Zhang S. Motion induced error reduction by combining fourier transform profilometry with phase-shifting profilometry. Opt Express 2016;24(20):23289–303.
[64] Dai J, An Y, Zhang S. Absolute three-dimensional shape measurement with a known object. Opt Express 2017;25(9):10384–96.
[65] Lohry W, Zhang S. High-speed absolute three-dimensional shape measurement using three binary dithered patterns. Opt Express 2014;22(22):26752–62.
[66] Li Y, Zhao C, Qian Y, Wang H, Jin H. High-speed and dense three-dimensional surface acquisition using defocused binary patterns for spatially isolated objects. Opt Express 2010;18(21):21628–35.
[67] Cruz-Santos W, Lopez-Garcia L. Implicit absolute phase retrieval in digital fringe projection without reference lines. Appl Opt 2015;54(7):1688–95.
[68] Guo H, Huang P. 3-D shape measurement by use of a modified fourier transform method. In: Proceedings of the 2008 SPIE international society for optical engineering, 7066; 2008. p. 70660E.
[69] Zhang S, Yau S-T. High-resolution, real-time 3-D absolute coordinate measurement based on a phase-shifting method. Opt Express 2006;14(7):2644–9.
[70] Su X, Zhang Q, Xiao Y, Xiang L. Dynamic 3-D shape measurement techniques with marked fringes tracking. In: Proceedings of the 2009 Fringe; 2009. p. 493–6.
[71] Cui H, Liao W, Dai N, Cheng X. A flexible phase-shifting method with absolute phase marker retrieval. Measurement 2012;45(1):101–8.
[72] Xiao Y, Su X, Zhang Q, Li Z. 3-D profilometry for the impact process with marked fringes tracking. Opto-Electron Eng 2007;34(8):46–52.
[73] Budianto B, Lun P, Hsung T-C. Marker encoded fringe projection profilometry for efficient 3d model acquisition. Appl Opt 2014;53(31):7442–53.
[74] Cong P, Xiong Z, Zhang Y, Zhao S, Wu F. Accurate dynamic 3D sensing with fourier-assisted phase shifting. IEEE J Sel Top Signal Process 2015;9(3):396–408.
[75] Zhang S. Phase unwrapping error reduction framework for a multiple-wavelength phase-shifting algorithm. Opt Eng 2009;48(10):105601.
[76] Feng S, Chen Q, Zuo C, Li R, Shen G, Feng F. Automatic identification and removal of outliers for high-speed fringe projection profilometry. Opt Eng 2013;52(1):013605.
[77] Huang L, Asundi AK. Phase invalidity identification framework with the temporal phase unwrapping method. Meas Sci Technol 2011;22(3):035304.
[78] Huang L, Asundi AK. Practical framework for phase retrieval and invalidity identification with temporal phase unwrapping method in fringe projection profilometry. Appl Mech Mater 2011;83:179–84.
[79] Wang H, Kemao Q, Soon SH. Valid point detection in fringe projection profilometry. Opt Express 2015;23(6):7535–49.
[80] Zhang C, Zhao H, Zhang L. Fringe order error in multifrequency fringe projection phase unwrapping: reason and correction. Appl Opt 2015;54(22):9390–9.
[81] Lu J, Mo R, Sun H, Chang Z, Zhao X. Invalid phase values removal method for absolute phase recovery. Appl Opt 2016;55(2):387–94.
[82] Chen F, Su X, Xiang L. Analysis and identification of phase error in phase measuring profilometry. Opt Express 2010;18(11):11300–7.
[83] Song L, Chang Y, Li Z, Wang P, Xing G, Xi J. Application of global phase filtering method in multi frequency measurement. Opt Express 2014;22(11):13641–7.
[84] Ding Y, Peng K, Lu L, Zhong K, Zhu Z. Simplified fringe order correction for absolute phase maps recovered with multiple-spatial-frequency fringe projections. Meas Sci Technol 2017;28(2):025203.